

OVERVIEW OF SOME ONERA RECENT ADVANCES IN ROTATING MACHINES NUMERICAL AEROELASTICITY

A.Dugeai¹, A.Placzek¹, Y. Mauffrey¹, S. Verley¹,

¹ Onera – The French Aerospace Lab
F-92322 Châtillon, FRANCE

alain.dugeai@onera.fr, antoine.placzek@onera.fr,
yann.mauffrey@onera.fr, simon.verley@onera.fr,

Keywords: turbomachine, aeroelasticity, multi-stage, coupling, Navier-Stokes.

Abstract: This paper presents the status of current development and research activities concerning the modelling of aeroelastic phenomena of rotating machines. A first insight will be given into the activities conducted in the frame of stage and multi-stage configurations of compressors. A second topic will be addressed concerning the development of methodologies for the taking into account of geometrical non-linear structural behaviour in the modelling of static aeroelasticity of large fan blades. An overview of recent applications in the field of turbomachinery aeroelasticity will be drawn. Perspectives of new activities will be given.

NOMENCLATURE

θ	azimuth angle	α	relaxation coefficient
N	number of sectors of the row	u	structural displacements
Φ	deformation mode shapes	w	aerodynamic field
M, D, K	structural mass, damping, stiffness matrices	σ_n	inter-blade phase angle
q	generalized coordinates	$X = \begin{bmatrix} u \\ w \end{bmatrix}$	fluid-structure variables
$F_A(t)$	aerodynamic force		

1 INTRODUCTION

The Aeroelasticity Modelling and Simulation research unit of ONERA develops and validates numerical methods for the prediction of the aeroelastic behaviour of aeronautical structures. This activity covers various applicative finalities such as military and civil aircrafts, aeronautical engines, and helicopters. This paper intends to present some recent advances conducted at ONERA concerning the prediction of the aeroelastic behaviour of aeronautical rotating machines, such as fans, contra-fans, and open-rotors.

Concerning turbomachinery aeroelasticity, a large effort has been put over the last decades on the development of numerical methods for the prediction of unsteady aerodynamic forces, in the context of vibrating isolated rows, either using a sector reduction or a full 360° model. Moreover, the focus has been initially set on the modelling of purely linear structure of blades, either for flutter or forced response prediction.

However, in the trend of global reduction of the impact of aeronautical systems on environment, very stringent constraints are put on Aircraft and Engine manufacturers in order to meet ACARE 2020 objectives, in order to reduce noise emission and drastically improve energetic efficiency. Compared to 2005 figures, the target levels of emission reduction are as high as 50% for CO₂, 80% for NO_x and 50% in terms of noise emission. In this context, the external dimensions of aeronautical engines are getting larger and larger, in order to reach higher bypass ratios and thus higher efficiencies. Therefore, the blade radius of fans and open-rotors are increasing and moreover, new materials are implemented such as composite materials.

New challenges arise for the prediction of the aeroelastic behaviour of fan blades due to larger sizes and flexibilities. As a consequence, a new need emerges for the taking into account of non-linear modelling of the blade structure. On the other hand, the need for a better modelling of the complexity of turbomachines for aeroelasticity becomes stronger, and in particular, the taking into account of stage and multi-stage configurations involving unsteady interactions due to rotation and vibration.

In this paper, a first section will be devoted to the presentation of some details concerning the aerodynamic and aeroelastic solver *elsA*, developed by ONERA, which has been implemented in the presently discussed studies. A specific insight will be given into specific features implemented in the case of the sector reduction techniques used in the case of the aeroelastic modelling of turbomachines, implementing phase-lagged and multi-phase lagged boundary conditions. Another part will focus on the coupling features developed within the aeroelastic module in order to couple the *elsA* code with the structural solver MSC Nastran, enabling full non-linear static aeroelastic simulations. A second section of the paper will present some applications of these features.

2 AERODYNAMIC SOLVER *ELSA*

The present work has been conducted with the *elsA* solver, developed at ONERA (ONERA-Airbus-SAFRAN property). This project started in 1997 within the ONERA's aerodynamic department, and is now being developed by a large number of contributors from several departments inside ONERA, but also by industrial or academic partners, such as AIRBUS, SAFRAN, CERFACS, ECL/LMFA and CENAERO.

elsA is a multipurpose aerodynamic software dedicated to the simulations of external and internal flows for aircraft, turbomachinery, helicopter, propellers applications [1].

2.1 *elsA* aerodynamic solver features

elsA allows aerodynamic computations for compressible viscous and inviscid flows. It handles RANS and URANS equations with a large set of turbulence models ranging from algebraic to turbulent transport equations, including DRSM, DES and LES models which are now being implemented for some applications. Laminar-turbulent transition criteria are also available, including Menter transport equation model. Considering the meshing strategy, *elsA* has been initially developed as a multiblock structured grid solver. However, incoming developments have gradually been conducted to increase its capabilities, in order, first to take into account partially or non-coincident block joins, and then to handle Chimera overset grids. Patched grid and overset Chimera grids techniques may be implemented to overcome multiblock structured grids meshing issues for complex geometrical configurations. Moreover, hybrid structured/unstructured meshes capabilities are now available, which have

been extensively validated in particular for taking into account turbomachinery complex geometries including technological effects (cavities, injections, cooling devices, trenches). The use of Cartesian grids is available.

Motion and deformations of bodies may be taken into account for steady/unsteady applications. The finite volume approach is used for spatial discretization in connection with centered or upwind schemes (Jameson, Roe, Van Leer). Runge-Kutta or backward Euler time schemes are available. Local, global, dual and Gear time stepping schemes are implemented. Convergence may be accelerated using implicit techniques (IRS, LU factorization) and/or multigrid resolution schemes. For unsteady time-accurate simulations, Dual Time Stepping and Gear schemes are available. Considering rotating machinery problems, relative frame with either relative or absolute variables formulations may be used (turbomachinery, helicopter, propellers). Parallelization is achieved through the distribution of mesh blocks over a set of processors. As far as unsteady computations are concerned, elsA is able to handle mesh deformation using an ALE formulation of flow equations.

2.2 elsA aeroelastic module

The Aeroelasticity Modelling and Simulation research unit of ONERA has been developing within the elsA solver a specific module for solving aeroelastic problems, either in static or in dynamic. A general framework has been developed in the optional “Ael” subsystem of elsA ([2], [3], [4], [5]) over the last few years, in order to extend elsA to different kinds of static or unsteady aeroelastic simulations (Figure 1).

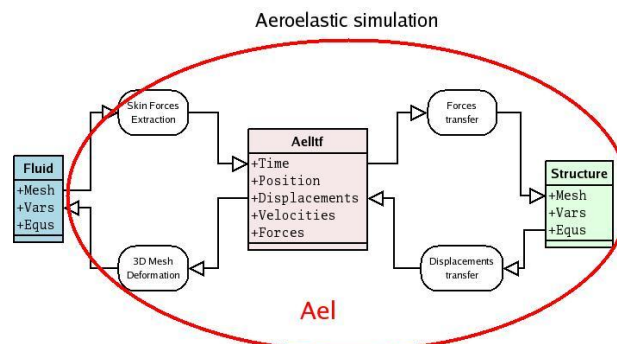


Figure 1 - elsA/Ael aeroelastic subsystem

The purpose of these simulations is the prediction of the in-flight static or dynamic behavior of flexible aerodynamic structures and their aeroelastic stability. This “Ael” subsystem gives access in a unified formulation to different types of aeroelastic simulations, compatible with the flow solver features. The available simulations include non-linear and linearized harmonic forced motion computations, static coupling and consistent dynamic coupling simulations in the time-domain. Harmonic balance method is also implemented for periodic forced motion simulations.

In the Ael module however, only a simple linear structural behaviour is assumed and implemented. Various kinds of linear structural modelling are available (“reduced flexibility matrix” for static coupling, modal approach, or full finite element structural model). In addition to the specific aeroelastic simulation driver, the elsA/Ael module basically integrates three main subsystems: a module for data transfer between fluid and structure solvers (including loads and displacements components), an integrated static and dynamic linear structural solver and a 3D fluid mesh deformation tool.

Transfer of displacements and loads between the structure and the fluid are based on the exchange of generalized coordinates and forces in the case of the modal approach, whereas it uses specific interpolation or smoothing techniques, the nearest neighbor or virtual work principle based techniques for the finite element approach. Concerning the important issue of 3D fluid mesh deformation, several methods are currently implemented such as described in the next paragraph.

Time consistent unsteady aeroelastic simulations are conducted using dual time stepping or Gear methods.

These simulations allow for the evaluation of the aeroelastic stability of aeronautical structures either in weakly coupled or strongly coupled strategy. In the weak coupling case, the motion of the structural model is prescribed as a single harmonic motion or a combination of harmonic motions, which can be rigid ones or following its natural vibration modes Φ . The computation is run over several periods of vibration in order to get the unsteady aerodynamic response to a forced motion of the structure. The aerodynamic temporal response of the fluid gives access to unsteady pressure distributions on the model surface, and may be integrated to get unsteady aerodynamic loads over the structure. In the purpose of linear stability analysis for flutter, these pressure distributions may be projected on the modal basis shapes, to get unsteady generalized aerodynamic forces $\Phi^T F_A(t)$ which are prescribed on the right hand side of the modal projected structural dynamics equation:

$$\Phi^T M \Phi \ddot{q} + \Phi^T D \Phi \dot{q} + \Phi^T K \Phi q - \Phi^T F_A(t) = 0$$

A first harmonic analysis of the unsteady forces is performed to study in the frequency domain the aeroelastic stability of the fluid-structure coupled system. Flutter response is classically analysed using p-k stability method.

In the strong coupling case, the structural dynamics equation is directly solved in the time domain during the unsteady aerodynamic computation, using a Newmark resolution scheme. At each physical time step, aerodynamic forces and elastic forces are balanced using an additional coupling loop and the procedure gives access to the unsteady evolutions of the structural variables and of the aerodynamic field as well.

Several mesh deformation techniques are also implemented in the Ael module. A first technique is based on the resolution of an equivalent linear elastic continuous medium equivalent problem, whose boundary conditions prescribe the displacement of the aerodynamic grid at aeroelastic interfaces. A 8-node hexahedral finite element approach is used to discretize the aerodynamic grid mesh deformation problem. The local stiffness matrix is computed approximately, using a one point Gauss integration procedure, specifically corrected for Hour-glass spurious modes treatment. The static equilibrium of the discretized system leads to the following linear system:

$$K_{ii} q_i = -K_{if} q_f$$

where q_i and q_f are respectively the computed and boundary prescribed displacement vectors. As the stiffness matrix is positive definite, the system is solved using a pre-conditioned conjugated gradient method. For elsA the technique is implemented in the case of multi-block structured grids. The full mesh deformation is defined as a sequence of individual block deformations.

Boundary conditions are set to impose zero or prescribed displacement values, to move on a plane, on the local surface boundary or along or normally to a prescribed vector, and to get deformations continuity through block interfaces. In order to fulfil boundary conditions, the conjugated gradient algorithm is modified.

The resolution procedure is kept compatible with the boundary conditions in iteratively projecting the solution and search direction vectors in the proper linear subspace. However, performing structural static deformation computations on the full aerodynamic grid is expensive, and reduction techniques are implemented in order to solve the structural problem on a coarse grid, by packing cells, especially in the boundary layer regions where the aerodynamic discretization is extremely dense.

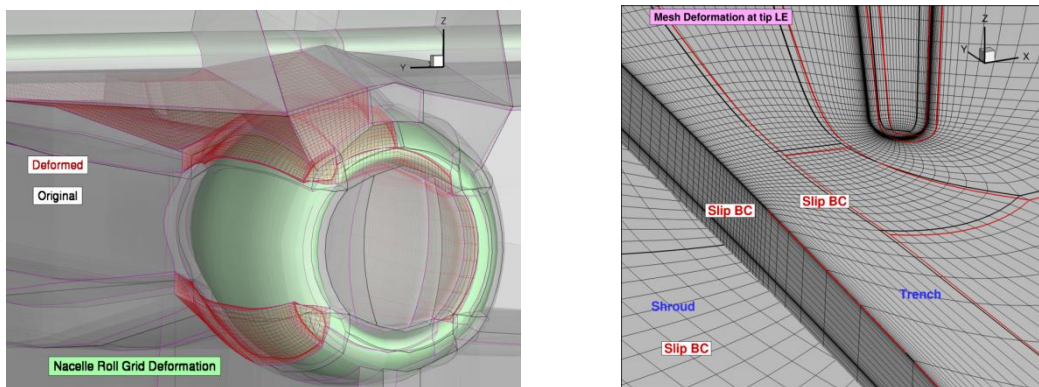


Figure 2: Mesh deformation examples using elastic analogy: oscillating nacelle (a), axial compressor with trench clearance at shroud (b)

The structural analogy method is very versatile and is used for a large range of applications: turbomachines, aircrafts, helicopters, propellers and CRORs. The implemented mesh deformation procedure has been validated for use with Chimera grids, and is now being fully parallelized in the current elsA version.

An alternate mesh deformation method based on a mixture of Inverse Distance Weighting (IDW) method and TransFinite Interpolation (TFI) is also available in the case of multiblock structured configurations. IDW is implemented in order to prescribe displacements on block boundaries, and the displacements of internal block nodes are obtained from the boundaries using the TFI algorithm. New developments are currently conducted in order to implement a Quaternion based mesh deformation method in a robust and efficient way, using a Fast-Multipole Method accelerated IDW algorithm.

3 AEROELASTICITY DEVELOPMENTS FOR STAGE/MULTISTAGE TURBOMACHINE CONFIGURATIONS

3.1 Reductions for aeroelastic problems for cyclic periodic configurations

The aeroelastic module of elsA is implemented for the study of the aeroelastic stability of aeronautical structures, using a weakly coupled approach. In this case harmonic forced motions simulations are conducted, in order to obtain the generalized aerodynamic forces giving access to the aerodynamic damping. In the case of turbomachines, the geometric and structural configurations are assumed to exhibit a cyclic periodicity. This property allows for channel reduction formulations, either for the structural dynamic behaviour, or for the aerodynamic flow field.

3.1.1 Phase lagged boundary conditions

The phase lagged boundary condition holds in case of a single purely time-periodic phenomenon. In the case of cyclic symmetric structures, the deformation of the structure may be represented in the linear case as a combination of nodal-diameter mode shapes, for which successive blade vibrates at a specific inter-blade phase angle. The vibration of the row may be described by the duplication of a reference sector, taking into account the phase shift induced by a specific inter-blade phase angle. Due to the azimuthal periodicity of the deformation, a generic displacement field may be represented as a Fourier series in azimuth θ , and taking into account the cyclic symmetry of the row (made of N identical sectors), it can be written as the sum of so-called diameter modes u_n as written below:

$$u(r, \theta, z, t) = \text{Re}\left(\sum_{n=0}^{N-1} u_n(r, \theta, z, t)\right)$$

Each nodal-diameter component exhibits a boundary condition between the values of u_n at the upper and lower boundaries of the sector, associated with a specific value of inter blade phase angle σ_n , which can be expressed as follows:

$$u_n(r, \theta + \beta, z, t) = u_n(r, \theta, z, t)e^{i\sigma_n} \quad \text{with} \quad \sigma_n = n\beta$$

where β is the azimuthal extension of the sector.

In the case of an aeroelastic simulation of harmonic forced motion following a n-nodal diameter mode of vibration Φ_n , the temporal evolution of the reference sector displacements may be expressed as:

$$u_n(r, \theta, z, t) = \Phi_n(r, \theta, z)e^{i\omega t}$$

The phase-lagged boundary conditions in this case may be expressed in the time domain as a time-shift of duration $\frac{\sigma_n}{\omega}$, corresponding to the propagation time of the deformation/unsteady flow component rotating wave through the sector:

$$u_n(r, \theta + \beta, z, t) = \Phi_n(r, \theta, z)e^{i\omega t}e^{i\sigma_n} = \Phi_n(r, \theta, z)e^{i\omega(t + \frac{\sigma_n}{\omega})} = u_n\left(r, \theta, z, t + \frac{\sigma_n}{\omega}\right)$$

These properties extend to the forced response of the fluid system, which also exhibits the same n-nodal diameter azimuthal periodicity at convergence of the process.

$$\begin{aligned} w_n(r, \theta + \beta, z, t) &= w_n(r, \theta, z, t)e^{i\sigma_n} \\ w_n(r, \theta + \beta, z, t) &= w_n\left(r, \theta, z, t + \frac{\sigma_n}{\omega}\right) \end{aligned}$$

This condition is implemented in elsA for aeroelastic simulation of harmonic forced motion as the so-called ‘‘chorochronic’’ boundary condition, using a Fourier decomposition process in the time domain, due to the time-periodic features of the phenomenon. This Fourier analysis is conducted at each time step at upper and lower boundaries of the sector, and characteristic relations are used to establish the equilibrium with the flow reconstructed at a shifted time on the other boundary using the current Fourier coefficients.

3.1.2 Extension of the phase lagged boundary conditions in the case of stage aeroelastic simulations

In the case of harmonic forced motion simulations conducted on a turbomachine stage configuration, two different periodic phenomena are superimposed. The first one is the effect of periodic blade passage of the opposite row, and the second is the rotating wave of deformation induced by the propagation wave of the considered n-nodal deformation mode shape. Due to different pulsations, the resulting unsteady flow field is basically not periodic in

time. Using an assumption of small perturbations, the unsteady flow field may be represented as a summation of rotating perturbation waves due to both phenomena. Following Tyler and Sofrin [6], we may approximate the unsteady flow as

$$w(r, \theta, z, t) = w_0(r, \theta, z) + \sum_{p=0}^{N_{sp}-1} w_p(r, \theta, z, t)$$

where w_p is a specific rotating wave, whose characteristics are a specific wave number κ_p (or nodal diameter) and a specific pulsation ω_p . Each rotating wave exhibits a specific rotation speed $c_p = \frac{\omega_p}{\kappa_p}$, and phase-lagged boundary conditions may be applied at upper and lower boundaries of the considered row sector, with specific phase angle and/or time shift for each rotating wave ([7]).

The Fourier decomposition/reconstruction process at sector boundaries is applied here for each rotating wave components in order to prescribe the proper boundary conditions.

	Sector angle	Wave number	Pulsation	Phase shift	Time shift
	$\beta = \frac{2\pi}{N}$	κ_p	ω_p	$\sigma = \kappa_p \beta$	$\tau = \frac{\kappa_p}{\omega_p} \beta$
Blade passing		Number of opposite blades N_{opp}	Pulsation of blade passing $N_{opp} \Delta\Omega$	$N_{opp} \beta$	$\frac{\beta}{\Delta\Omega}$
Vibration		Nodal diameter n	Vibration pulsation ω	$n\beta$	$\frac{n\beta}{\omega}$

Table 1: Frequency-time relationships for a rotating wave component

For better robustness, a relaxation procedure is applied at each time step on the Fourier coefficients of each rotating wave included in the simulation. These boundary conditions are implemented in the following unsteady simulations presented here after in section 4.

3.2 Fluid-structure coupling between elsA and MSC NASTRAN

In many aeroelasticity problems, the structure may be classically assumed to behave linearly. However, in some cases, the linear structure assumption is no longer valid. This is the case when geometric non-linearities such as large displacements are to be considered, for example for highly flexible wings, or in the turbomachine case, for rotating blades of large dimensions, such as large propellers, open-rotors or UHBR fan blades.

Therefore, new solutions for coupling non-linear aerodynamics and non-linear structural models are to be considered. The fluid-structure problem can be formulated as a coupled field problem, where the solutions are coupled only at the boundary interfaces between the fluid and the structure ([8]). It is then possible to run separate solvers for the flow computation and the structure computation, and to reach a coupled solution by exchanging information at the common fluid-structure boundaries.

The currently implemented mechanism used for coupling elsA and an external CSM solver basically relies on the exchange of data at the aeroelastic interface, using CGNS standard compliant interface. The aeroelastic module features of elsA are used, except for the internal

structural model resolution which is externalized. The standard aeroelastic simulation is interrupted at each coupling step, and aerodynamic forces located at an embedded reduced structural model (either modal or finite element) are computed using the Ael module integrated force transfer methods. This data is extracted and provided to the CGNS memory data base, which in turn is processed by an external Python coupling script in charge of the communication with the external structural solver. Nastran is run in non-linear mode, using the SOL400 solution, taking into account following forces for the prescription of aerodynamic forces at each time step. At the end of the structural step, displacements on the reduced structural model are sent back to elsA and transferred to the aeroelastic interface. 3D aerodynamic mesh deformation is then performed before going on with new fluid resolution iterations. This architecture has been developed for the purpose of running aeroelastic simulations coupling elsA with the non-linear commercial structural solver MSC Nastran. To do that, a specific interface written in C language and based on the use of the OpenFSI module of Nastran has been developed and coupled with a Python interface (Figure 3).

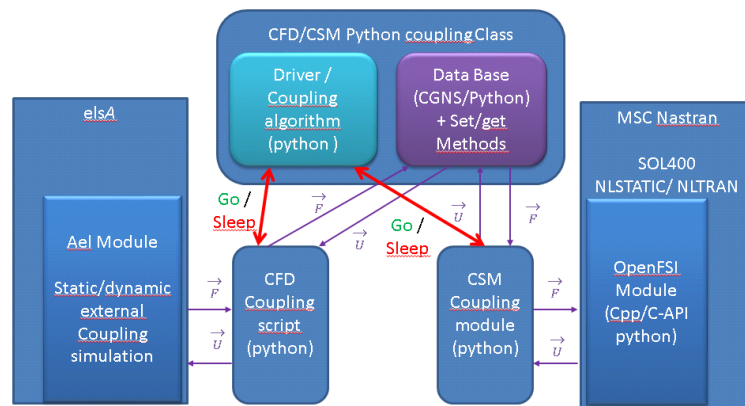


Figure 3: Current Coupling architecture with MSC Nastran SOL 400

The coupling strategy is basically a fixed point method, potentially requiring the use of a relaxation procedure to ensure convergence.

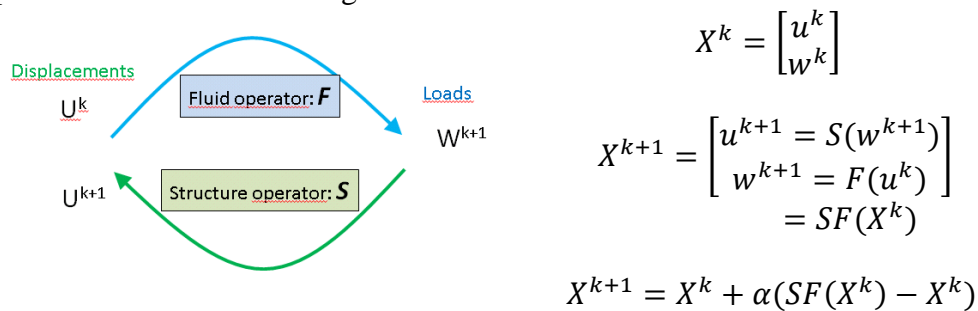


Figure 4: Fluid-structure fixed-point algorithm

This mechanism has been implemented in the case of static hot shape predictions of UHBR and open-rotor fan blades. In this case, the non-linear structural modelling is mandatory due to effect of high speed rotation inducing additional stiffness terms and centrifugal forces.

4 APPLICATIONS

This section presents an overview of several applications activities implementing the previously detailed aeroelastic capabilities of elsA. Two applications concern the CFD-CSM

coupling procedure which has been used in the frames of the ENOVAL and ADEC European projects. Two other items are presented concerning the use of the phase-lagged and multi-phase lagged sector reduction capabilities for stage and multi-stage configurations, during the COBRA Europe-Russia collaboration and in the frame of the elsA-ASO development program with SAFRAN.

Caution: Due the confidential features of the presented industrial applications, figures have been suppressed from specific plots.

4.1 ENOVAL UHBR fan Flexible operating map prediction

An application of the developed simulation tools based on the coupling of elsA/Ael and MSC/Nastran has been performed for the purpose of computing the hot-shape of a UHBR fan-blade in the framework of the European project ENOVAL.

The implemented model is shown in Figure 5. On the left side, a view of the aerodynamic sector domain is displayed. The middle plot presents the selected reduced structural model defining the aeroelastic transfer model. On the right part, the full Finite Element model used for static non-linear large displacements structural simulation with Nastran is plotted.

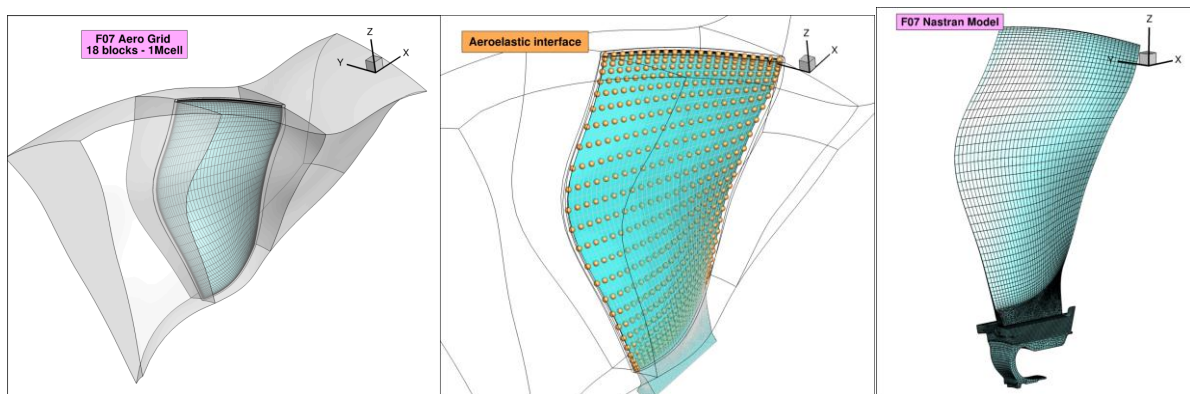


Figure 5: ENOVAL fan aeroelastic model

The present fully non-linear coupling algorithm has been implemented for the computation of the massflow to pressure ratio characteristic map of the fan for the 100% of nominal speed line. Contrary to the standard procedure where a unique shape (computed on the nominal operating line) is used for the evaluation of the performance of the fan, the coupled fluid-structure equilibrium is evaluated at each point of the characteristic line, which means that a specific shape is computed at each point of the map, due to modification of the pressure loads.

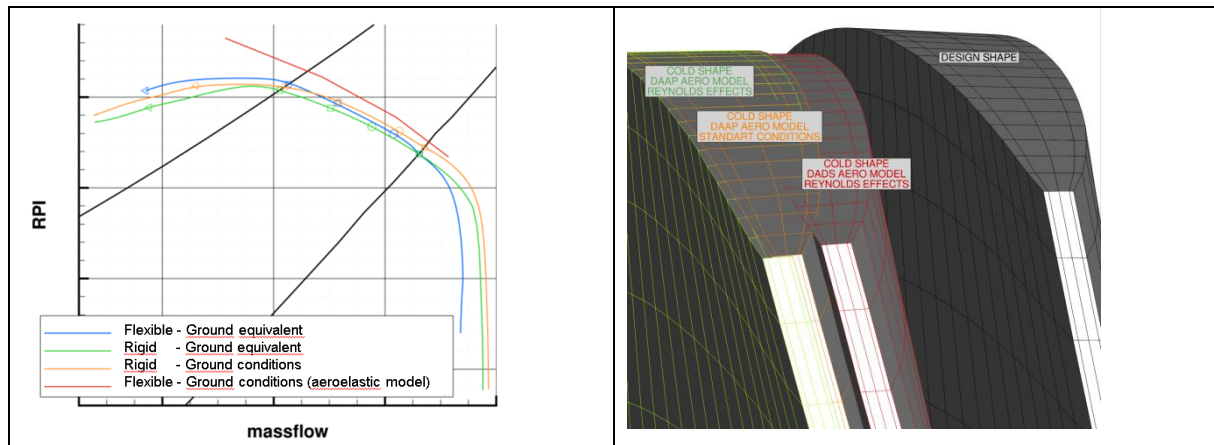


Figure 6: Flexible characteristic line at 100% N_n (left) – Blade tip deformation (right)

The elsA solver is implemented using the Smith k-1 turbulence model, on a aerodynamic grid including the Outlet Guide Vane (OGV), of 1.6 Mio cells. The fan performance for ground conditions computed with flexible shapes are compared to those obtained in rigid mode in Figure 6.

Reynolds effects are taken into account in comparing aerodynamic loads classically obtained with flight conditions and extrapolated to ground conditions (in green and blue) and those directly computed with ground conditions, inducing differences in Reynolds number (orange and red). The different models show an influence on maximum pressure ratio and blocking massflow, which may be of substantial importance on design.

However one bottleneck for the generalization of the procedure for the whole fan map is the robustness of the mesh deformation process, because of large variations of fan shape, especially considering the fan tip gap region, which may vary considerably, inducing large mesh stretching (Figure 6, right). One clue for the extension of the procedure will be the improvement of mesh deformation technique robustness and efficiency.

4.2 CleanSky II / ADEC CROR non-linear hot shapes prediction

The present CFD-CSM coupling procedure has also been implemented in the framework of the CleanSky 2 ADEC European project, for the purpose of the prediction of fan blades hot shapes of the AIPX7 Airbus CROR model, tested at the Z49 rig in the S2Ma ONERA wind-tunnel facility ([9],[10]).

For this study, non-linear structural modelling has been implemented in coupling elsA using the solution SOL400 of MSC/NASTRAN, in order to take into account geometric non-linear large displacements effects. In order to highlight the need of nonlinear structural modeling in hot shape prediction in this case, Figure 7, left shows a comparison between the blade displacements, in terms of bending (top) and twist angle (bottom), obtained using linear CSM (in blue) and nonlinear CSM (in orange) during hot shape computations for the front rotor blade, in comparison with the experimental data in dashed red lines. The selected operating point for this comparison is located at $M=0.75$, for a rotation speed of 4510 rpm, at 0° AoA. Linear approach over estimates both blade bending and blade twist by a factor 2. In comparison, nonlinear results are very well fitting the experimental data.

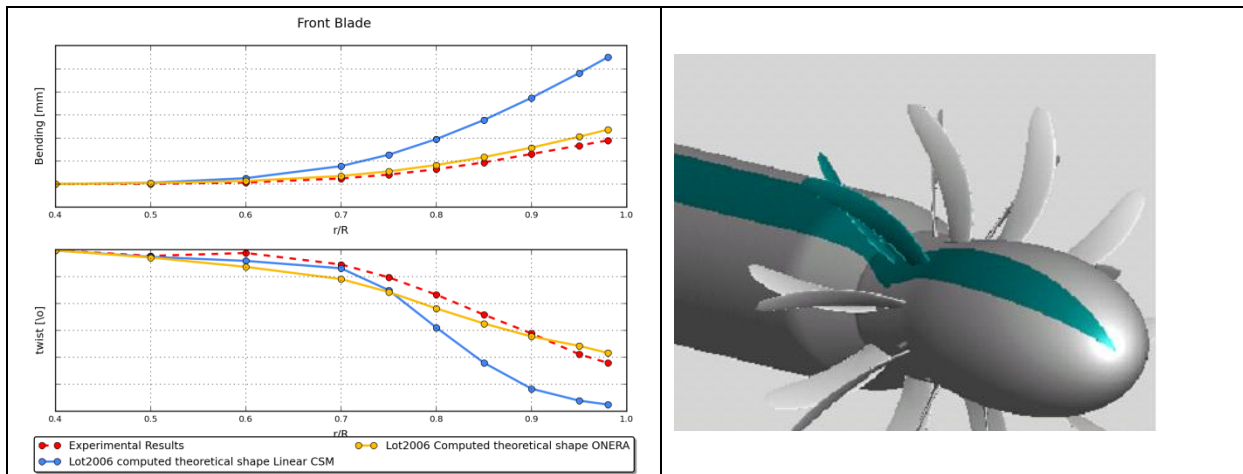


Figure 7: AIXP7 at Z49 rig - CFD-CSM coupling simulation @ cruise conditions $M=0.75$
 Twist and bending deformations non-linear vs linear structure (left), CROR Model and sector (right)

During this study, manufactured blade shape measurements were performed by Airbus on the Z49 test facility. A part of the work was dedicated to evaluate the consequences of manufacturing uncertainties on numerical hot shape prediction. Figure 8, left, shows blade deformation comparison in term of bending (top) and twist (bottom) versus blade span for the front rotor blade.

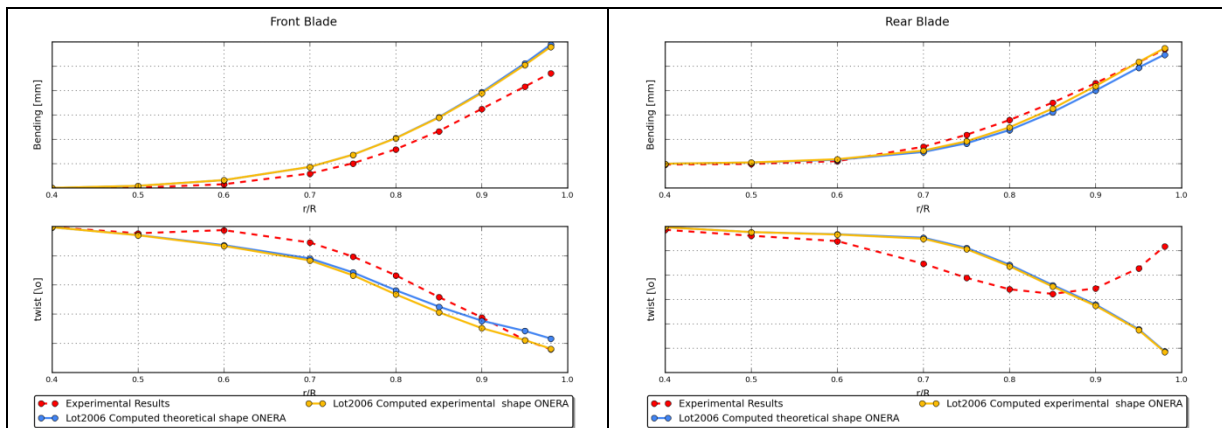


Figure 8: AIXP7 at Z49 rig - CFD-CSM coupling simulation @ cruise conditions $M=0.75$. comparison between manufactured shape and CAD shape blade deflections

The blue and orange curves respectively depict the computed deflection using CAD shape and experimental shape. If fair agreement with experimental data is observed for both models, taking into account the real manufactured shapes improves the results for twist angle in the blade tip region. On the right part of this figure are shown the results for the rear blade. Experimental and numerical results are in good agreement concerning the bending, but major discrepancies are observed concerning the twist. It seems that a physical phenomenon is missed by the numerical simulations. First investigations tend to show that the blade vortex interaction may have an impact on the blade displacements, but the mixing plane boundary conditions prescribed at front and rear rotor interface which forces a steady solution in the CFD computations does not allow for the taking into account of this unsteady interaction.

Work is now ongoing in order to take into account this phenomenon using 360° simulations, and to perform numerical restitutions of unsteady blade deformations for experimental operating points with nonzero AoA.

4.3 COBRA contrafan aeroelastic analysis

ONERA is the coordinator of the COBRA “Innovative counter rotating fan system for high bypass ratio aircraft engine” Europe-Russia cooperative research project, in collaboration with SAFRAN, DLR, CIAM and COMOTI. The purpose of COBRA is to use technology breakthroughs to overcome the insufficient noise performance of the counter-rotating fan tested in VITAL EU FP6 Program. This will be achieved through exploring higher by-pass ratio (15-25) resulting in much lower blade tip speed and blades count. The global objective is to overcome the aerodynamic efficiency obtained by the VITAL design.

This section presents the activity carried out as part of the workpackage WP4 of COBRA, to assess the aeroelastic stability of the version V4bis of the VITAL contrafan designed during the project. Figure 9 presents a view of the modelled geometry (structure and aerodynamic grids). Both front and aft fans are fully metallic and made of titanium.

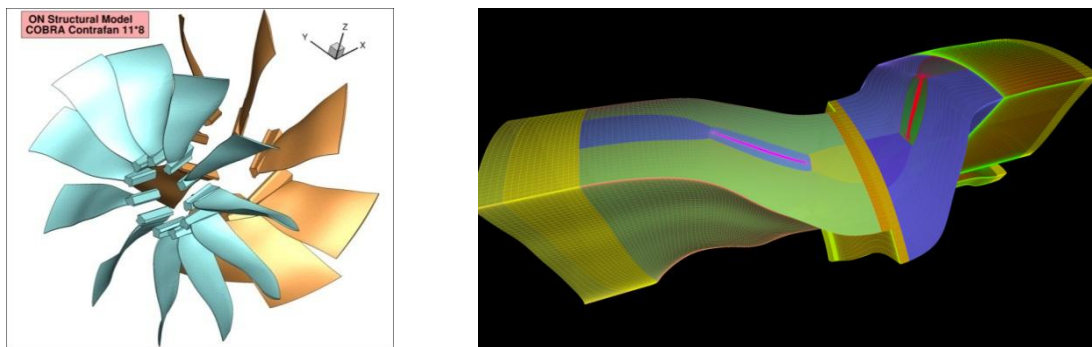


Figure 9: COBRA: Structural models (left), Aerodynamic elsA Grid (right)

For aeroelastic simulations, finite elements grids have been generated for both blades using an in-house software, and connected to blade disk models provided by COMOTI. NASTRAN SOL106 non-linear static analysis, followed by a normal mode analysis, is performed to get the eigenmodes basis relative to the non-linear deformed shape including large displacement effects. Figure 10 illustrate the obtained mode shapes at nodal diameter 0, at aerodynamic design point, for the front blade model (left) and the aft one (right).

Aerodynamic steady computations have been performed using elsA and compared to equivalent results obtained by DLR. Some discrepancies have been observed in terms of max massflow values, as well as max pressure ratio near stall which are still not well understood (Figure 10, right).

Numerical simulations have been conducted using elsA in order to study the aeroelastic stability of the contrafan. In this case sector reduction has been implemented, with phase-lagged boundary conditions, assuming no unsteady aerodynamic interactions between both fans. Therefore an azimuthal mixing plane boundary condition has been applied at the row interface, and a single aeroelastic rotating wave has been implemented in each row domain.

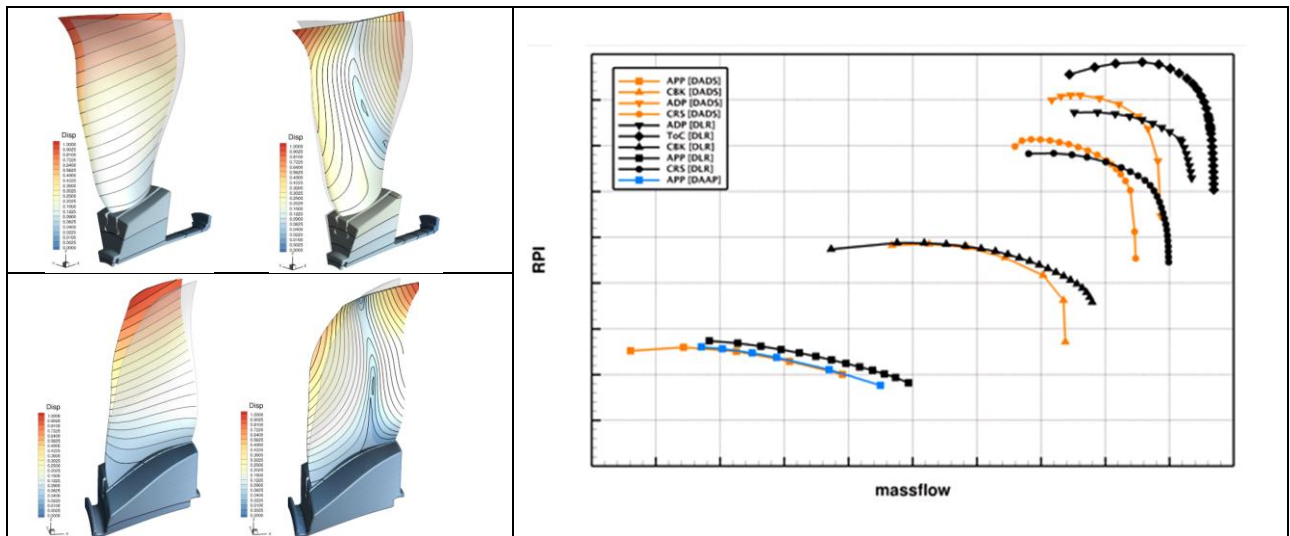


Figure 10: 1F, 1T modes @ nodal diameter 0, ADP (front (top) & aft blades (bottom)) – fan map (right)

Aeroelastic simulations have then been conducted for 3 operating point (Approach, Cutback and Design point). The Dual Time Stepping scheme is implemented for the time-consistent resolution of the aerodynamic response to a harmonic forced motion following modal vibrations of each blade rows. 26 periods of vibrations are computed in order to reach a conveniently converged periodic solution. First and second bending and first torsion modes are investigated for each blade row, along with inter-blade dephasing patterns matching with 7 values of nodal diameter, requiring the use of phase-lagged boundary conditions. A set of 117 non-linear deformable unsteady aeroelastic URANS simulations have been run on 32 cores, each of them corresponding to a typical wall clock computation time of 13 hours.

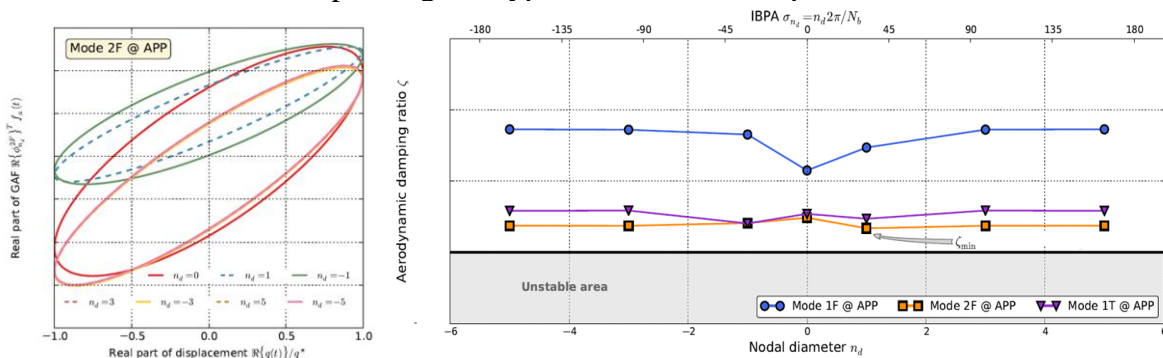


Figure 11: Approach case - Row 1: GAF Lissajous curves of mode 2F (left), aerodynamic damping evolution vs nodal diameter for 1F, 2F and 1T modes (right)

Figure 11 presents on the left side the evolution of generalized aerodynamic forces versus excitation generalized coordinate (Lissajous curve), illustrating the properly converged state of the simulations, conducted here for the 2nd bending mode of the first row, for the Approach operating point and for various inter-blade phase angle values. The harmonic analysis of generalized forces leads to the extraction of the corresponding damping which is plotted on the right side of the figure, for the same operating point, and for the three selected modes shapes (i.e. first and second bending and first torsion). The minimal value of aerodynamic damping is obtained in this case for second bending at nodal diameter 1. However, the full configuration stays clear of flutter in any case.

4.4 ASTEC2 multi-stage compressor multi-phase-lagged analysis

Multi-phase-lagged boundary conditions have been implemented ([11],[12]) in the case of multi-stage axial compressor configuration provided by SAFRAN HE, composed of 6 rows, including a structural strut row, an inlet guide vane and two rotor/stator stages. Due to the high number of blades of the full 360° degree configuration (131 blades), a reduced modelling is mandatory for aeroelastic unsteady configurations in order to keep within acceptable CPU time resources. Therefore, a single sector reduction has been used, including aerodynamic interactions between adjacent rows, with the implementation of the multi-phase lagged boundary condition.

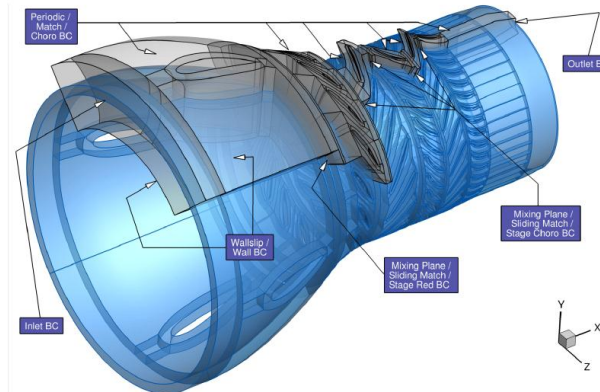


Figure 12: SAFRAN HE multistage compressor configuration: sector reduction vs 360° full annulus slice model

Several models have been implemented for the purpose of the validation of the proper use of interface boundary conditions between rows 1 and 2, and of multi-phase-lagged boundary conditions setup.

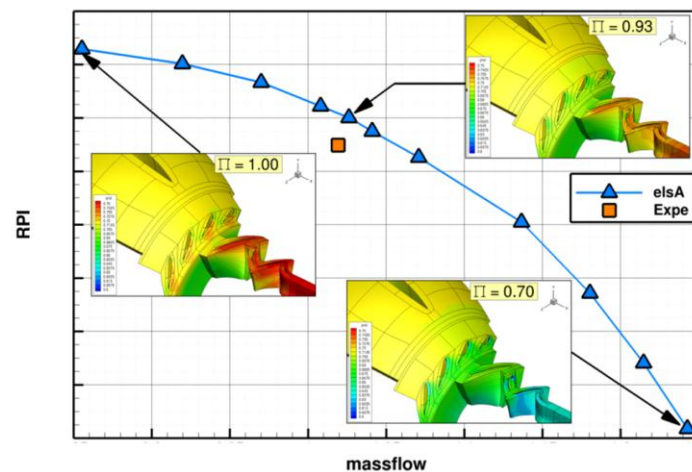


Figure 13: Compressor map for the 3D sector model

A full 360° annulus slice model (6.5 Mio cells) and a corresponding sector reduction model (0.54 Mio cells) have first been built, in order to cross-validate at lower cost the implementation of the multi-phase lagged boundary conditions. For the 3D configuration, only a single passage aerodynamic model has been made, including 164 blocks and roughly 16 Mio cells.

A reference unsteady simulation is performed with the full annulus 2.5D multistage configuration using 64 processors. The simulation is run for 14.4 revolutions so that a periodic state can be reached for a total wall-clock time of about 10 days. This simulation is compared to the equivalent single passage simulation performed using multi-phase lagged boundary conditions to allow for the propagation of blade-passage perturbations rotating waves. In this case, a maximum of two spinning modes is considered, corresponding to the rotating waves produced by the blade passing of the two adjacent rows with nonzero relative speed. For all spinning modes, 48 harmonics are computed and a relaxation factor is set either to 0.5 or 0.1. Because of the small value of the relaxation coefficient, the convergence is longer than for the full annulus simulation but a periodic state is reached before the end of the 14.4 revolutions. The computation is run on only 14 processors, for a global wall-clock time of 2 days and 8 hours.

Figure 14 presents on the left the pressure time history recorded on a numerical sensor located on the R1 blade (top left) and in the R1 channel (bottom left). The 360° slice-reduction results are compared as a reference to the sector reduction solution using the multi-phase-lagged condition.

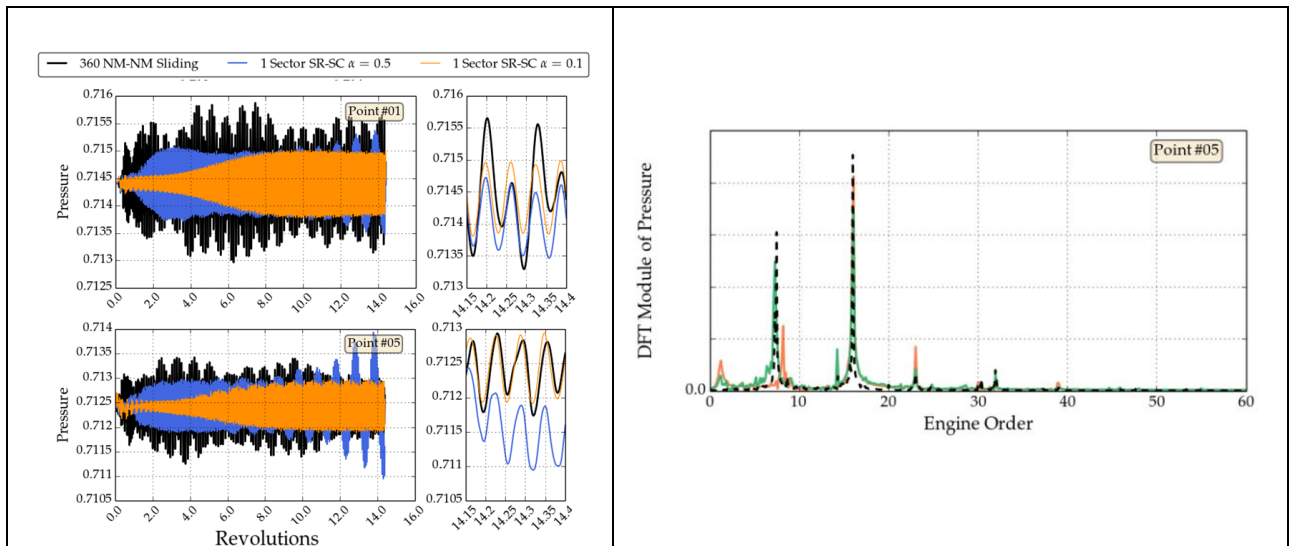


Figure 14: Pressure sensors history on R1 blade (top left) – in R1 channel (bottom left), Frequency content in R1 channel for 3 op. points (right)

The agreement between both solutions is visible, in terms of amplitude and global frequency content. The blue curve corresponds to the multi-phase-lagged case, with the highest value of relaxation coefficient, which however leads to a divergence of the simulation. One can see on the right part of the plot that apart from an unexpected tricky frequency located at 7.5 EO, the spectral content is driven by the blade passage frequencies in the different blade rows, with the main contribution of the 16th EO and its first harmonic (32nd EO) in R1 and R2. In blade row R3 the 16th EO due to the passage of $R2 > R3$ and the 29th EO due to the passage of $R4 > R3$ are dominating, with the additional 45th EO induced by the combination of the 16th and 29th EO.

It must be pointed out that a small relaxation factor (0.1) is necessary to ensure the robustness of the multichorochronic approximation for long time simulations and to avoid the apparition of spurious frequencies. Moreover, the full annulus model response exhibits an asynchronous frequency that cannot be captured by the multichorochronic approximation.

The unsteady rigid simulation has also been conducted in the case of the 3D single passage model (Figure 15). These simulations however have not been validated against the full 360° configuration equivalent results, for CPU cost clear reasons. Indeed, the simulation for the single sector model, is run with 90 processors to cover 20 revolutions for a total wallclock time of 13 days and 9 hours.

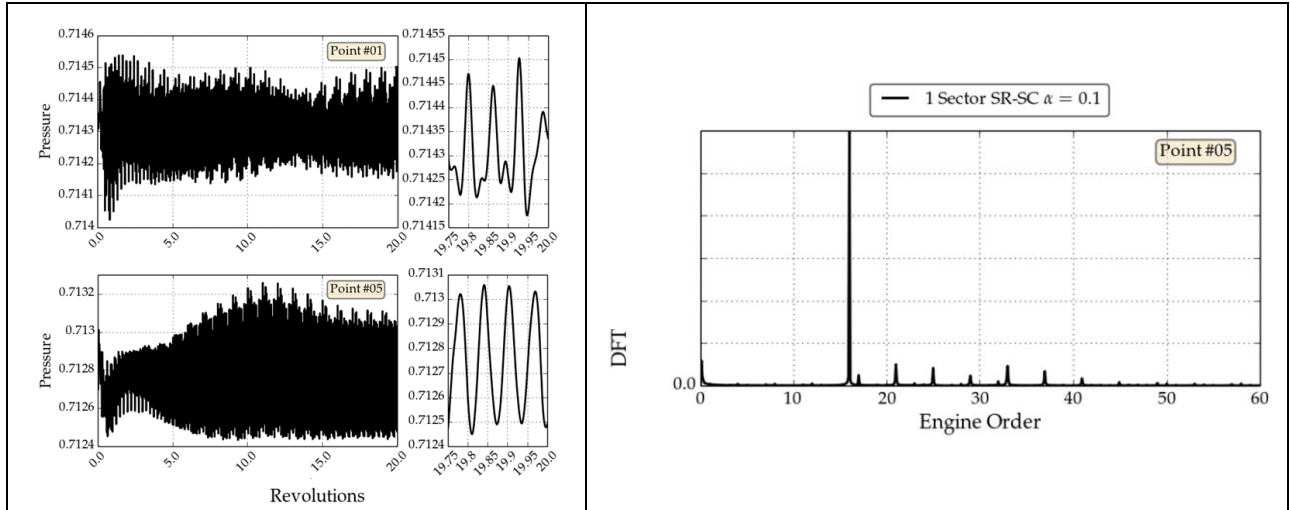


Figure 15: 3D sector model - Pressure sensors history on R1 blade (top left) – in R1 channel (bottom left), Frequency content in R1 channel (right)

The use of the multi-phased lagged boundary conditions approach for a multi-stage compressor configuration has been validated on a 2.5D slice reduction of the machine against full 360° model results. This validation however has been made in the rigid case, due to the lack of data for a proper aeroelastic validation setup. Moreover, a demonstration of the capability of the multi-phase-lagged approach has also been made on the 3D sector model. A fully aeroelastic validation implementing a modal vibration of a row, although already conducted on the more simpler VITAL contrafan configuration ([11],[12]), has still to be conducted on the ASTEC2 case, in order to fully validate the approach for aero-structure problems of multi-stage configurations.

5 PERSPECTIVES

Several activities are currently carried out in the Aeroelasticity Modelling and Simulation research unit of ONERA to address new topics concerning the aeroelastic behaviour of turbomachines. One main issue concerns the prediction of the aeroelastic stability and of the forced response of turbomachines, especially fans, facing distorted inlet conditions. In particular, due to inhomogeneous total pressure and velocity at inlet, large levels of structural forced response may be observed, which must be studied for safety reasons. These conditions may occur, in various circumstances, such as cross-wind conditions, impinging wakes, boundary layer ingestion (BLI), or even interactions with ground induced vortices (Figure 16, left). In these cases, the basic assumption for cyclic symmetry retained for sector reduction modelling is questionable, and 360° modelling may be mandatory.

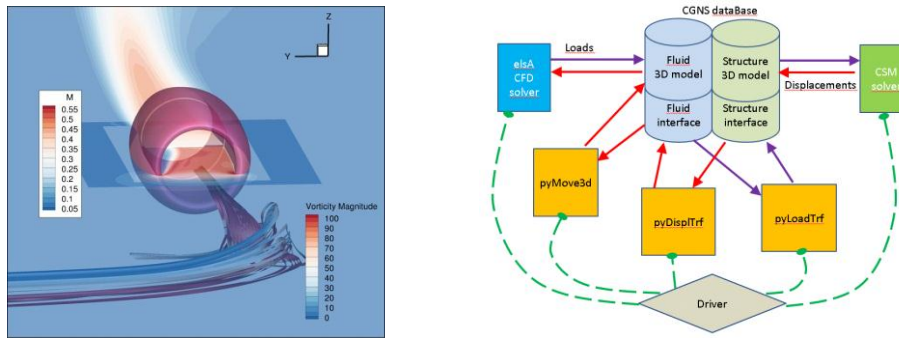


Figure 16: Fan-vortex interaction (left) - Targeted Fluid-structure modular architecture (right)

On the other hand, new activities are currently conducted in order to build a modular aeroelastic simulation environment, whose objective is to deliver new simulation capabilities in coupling several individual modules for the resolution of aeroelastic problems. This work intends to provide a tool versatile enough to extend the coupling solution currently available with elsA to other non-linear aerodynamic solvers (newly developed CFD2030 aerodynamic codes) and non-linear structural solvers. Such a tool will potentially provide the access to aerodynamic modeling alternative to URANS, such as LES, or Lattice-Boltzmann, and to innovative techniques such as Immersed Boundaries Method for aeroelasticity. Moreover, this modular architecture will allow to implement more easily new innovative algorithms for fluid-structure transfers and mesh deformation strategy, without costly additional elsA C++ Kernel development. This architecture will rely on CGNS compliant data model, specifically extended for fluid-structure coupling, and modular extensions using Python interfaces (Figure 16, right).

6 CONCLUSION

The aim of this paper was to present the status of current development and research activities concerning the modelling of aeroelastic phenomena of rotating machines. In a part 2, we have presented the basic capabilities of the elsA ONERA aerodynamic solver, and then those of the specific aeroelastic extension of elsA, Ael. In part 3, we have described specific functionalities recently implemented for unsteady weak coupling aeroelastic simulations of stage and multi-stage turbomachine configurations and for the non-linear coupling of the elsA non-linear aerodynamic solver and MSC/Nastran, implemented for non-linear large displacement static problems.

These functionalities have been implemented in several European and national project, such as COBRA, ENOVAL, CS2-ADEC and elsA/ASO.

One perspective of future work in the frame of aeroelastic problems of turbomachines concerns the taking into account of the impact of distorted inflow on aeroelasticity of fans and open-rotors, especially concerning forced response. This topic will be addressed in the ENOVAL European project framework in particular. Secondly, the extension of aeroelastic coupling capabilities to fully non-linear fluid-structure modelling is currently under construction and will provide larger modelling capabilities for aeroelastic problems.

7 ACKNOWLEDGEMENTS

The studies presented in this article, have been partially funded by Airbus, Safran and ONERA which are co-owners of the software.

8 REFERENCES

- [1] CAMBIER L., HEIB S., PLOT S., “The ONERA elsA CFD software: Input from Research and Feedback from Industry”, *Mechanics and Industry*, 14 (3), pp. 159-74, 2013.
- [2] DUGEAI A., Turbomachinery aeroelastic developments and validations using ONERA elsA solver, *International Forum on Aeroelasticity and Structural Dynamics*, 18-20 June 2007, Stockholm, Sweden
- [3] GIRODROUX-LAVIGNE P., “Fluid-Structure Coupling Using Chimera Grids”, *International Forum on Aeroelasticity and Structural Dynamics*, 21-25 June 2009, Seattle, USA.
- [4] DUGEAI A., MAUFFREY Y., SICOT F., “Aeroelastic capabilities of the elsA solver for rotating machines applications”, *IFASD 2011*, paper 079, Paris, June 2011
- [5] PLACZEK A., DUGEAI A., “Numerical prediction of the aeroelastic damping using multi-modal dynamically coupled simulations on a 360° fan configuration” *IFASD 2011*, paper 084, Paris, June 2011
- [6] TYLER J., SOFFRIN T. “Axial flow compressor noise studies”, *SAE Trans.*, 70:309–32, 1962.
- [7] GEROLYMOS G.A., MICHON G.J., and NEUBAUER J.. “Analysis and application of chorochronic periodicity in turbomachinery rotor/stator interaction computations”, *AIAA J.*, 18(6):1139–52, 2002.
- [8] ERRERA M.P., DUGEAI A., GIRODROUX-LAVIGNE P., GARAUD J-D., POINOT M., CERQUEIRA S., CHAINERAY G., “Multi-Physics Coupling Approaches for Aerospace Numerical Simulations”, *AerospaceLab n°2 – Issue 2*, pp. 1-16, 2011, ACLN - ONERA TP 2011-441
- [9] DUGEAI A., VERLEY S., “Numerical evaluation of CRORs dynamic loads induced by whirl flutter”, *3AF CEAS Greener Aviation*, Bruxelles, 2014, ACTI - ONERA TP 2014-209.
- [10] MAUFFREY, Y, GEERAERT, A, “CROR Blade deformation, part 2: Aeroelastic computations and comparison with experiments,” *IFASD International Forum on Aeroelasticity and Structural Dynamics*, June 28-July 2 2015, Saint Petersburg, Russia,
- [11] PLACZEK A., CASTILLON L., “Aeroelastic Response of a Contrafan Stage Using Full Annulus and Single Passage Models”, *Journal of Aeroelasticity and Structural Dynamics* Vol. 3, n° 2, pp. 1-30, 2014. ACLN - ONERA TP 2014-261.
- [12] PLACZEK A., “Aeroelastic damping predictions for multistage turbomachinery applications” *ICAS 2014, 29th Congress of the International Council of the Aeronautical Sciences*, Saint-Petersbourg, 2014, ACTI - ONERA TP 2014-588.

COPYRIGHT STATEMENT

The authors confirm that they, and/or their company or organization, hold copyright on all of the original material included in this paper. The authors also confirm that they have obtained permission, from the copyright holder of any third party material included in this paper, to publish it as part of their paper. The authors confirm that they give permission, or have obtained permission from the copyright holder of this paper, for the publication and distribution of this paper as part of the IFASD-2017 proceedings or as individual off-prints from the proceedings.